ICS PHYSICAL CHEMISTRY

DIVISI KIMIA FISIK

FULL PAPER

DOI: 10.34311/icspc.2021.1.1.10

Molecular Dynamics Simulation of Wetting Behavior: Contact Angle Dependency on Water Potential Models

Lukman Hakim,[a,b,c,*] Irsandi Dwi Oka Kurniawan[c], Ellya Indahyanti[c], Irwansyah Putra Pradana[c]

Received: January 15, 2021
Revised: February 2, 2021
Accepted: February 3, 2021

The underlying principle of surface wettability has obtained great attentions for the development of novel functional surfaces. Molecular dynamics simulations has been widely utilized to obtain molecular-level details of surface wettability that is commonly quantified in term of contact angle of a liquid droplet on the surface. In this work, the sensitivity of contact angle calculation at various degrees of surface hydrophilicity to the adopted potential models of water: SPC/E, TIP4P, and TIP5P, is investigated. The simulation cell consists of a water droplet on a structureless surface whose hydrophilicity is modified by introducing a scaling factor to the water-surface interaction parameter. The simulation shows that the differences in contact angle described by the potential models are systematic and become more visible with the increase of the surface hydrophilicity. An alternative method to compute a contact angle based on the height of center-of-mass of the droplet is also evaluated, and the resulting contact angles are generally larger than those determined from the liquid-gas interfacial line.

1 Introduction

Wettability is an inherent properties of solid surface that plays significant roles in diverse fields such as biological science [1–4] and material manufacturing [5–7]. From nature, the so-called “lotus effect" inspired the development of super hydrophobic surface that found its application in self-cleaning surfaces [7], corrosion inhibition [8], and rainproof mirror coating for automotive [9]. On the other side, nature also demonstrate the presence of super hydrophilic surfaces such as those in spider silks [2] and desert beetle's back [3]. This super hydrophilic surface is also actively investigated for its potential in oil/water separation [10] and biological cell adhesion [11]. One of the research pinnacle emanated from the wettability of solid surface is the reversible hydrophilic-hydrophobic switching surface [12–14]. In such materials, the wettability of surface is adjusted by altering the configuration of surface molecules through a simple physical or chemical treatment. Therefore, a molecular-level understanding of surface wettability has important implications to the development of surface technology.

The wettability of a solid surface is commonly quantified in term of the contact angle formed by a liquid droplet on the surface. A surface is defined to be hydrophobic when the contact angle of liquid droplet is larger than 90°, otherwise it is defined to be hydrophilic. A theoretical framework to describe the relation between a static contact angle of liquid droplet and the surface free energy is given by Young equation [15]. When the surface roughness is included in the picture, Wenzel model and Cassie model are the two most commonly employed framework [16]. In case of complete wetting, the contact angle is dynamically expressed as the advancing contact angle and the receding contact angle.

Molecular dynamics (MD) simulation is a powerful tool to obtain the microscopic details of atomistic system, and it has been widely used to investigate the physiochemistry of surface and the wetting behaviors [17–33]. One of the key issue in MD simulation is the potential models adopted to describe the interaction between molecules. The parameters of interaction between water molecules and surface atoms, such as σ_{ws} and ε_{ws}, are known to significantly affects the contact angle of water droplet, and thus have become the subject of fine tuning to reproduce the experimental observation [29,33]. On the other hand, the effects of the

[a] Elements Strategy Initiatives for Catalysts and Batteries, Kyoto University, Katsura, Kyoto 615-8520, Japan
[b] Graduate School of Engineering Science, Osaka University, Toyonaka, Osaka 560-8531, Japan
[c] Department of Chemistry, Faculty of Mathematics and Natural Science, Brawijaya University, Malang 65145, Indonesia
[*] Corresponding author: lukman.chemist@ub.ac.id

adopted potential model for water-water interactions to the contact angle measurement were scarcely reported. In one report, compared to the SPC/E water model, TIP3P was observed to give a smaller contact angle by 17.4°, while TIP5P was smaller by 4.1°[29]. The sensitivity of contact angle with the adopted potential models under various degree of surface wetting remains unexplored. In order to clarify this issue, MD simulations of a water droplet on a solid surface at various degrees of wetting are performed and three potential models for water: SPC/E[34], TIP4P[35], and TIP5P[36], are adopted for comparison. The potential models are known to reproduce many important properties of liquid water[37,38], along with certain set of limitations that characterize any rigid and non-polarizable models[39,40]. The solid surface is chosen to be structureless to exclude the additional roughness parameter. Two methods for determination of contact angles, one based on the liquid-gas interfacial line[29,33,41–43] and the other based on the height of center-of-mass of the droplet[32,44], are also evaluated.

2 Simulation methods

2.1 Simulation cell and potential models

The simulation cell is a cubic box with 20 nm length. The dimension is chosen to effectively remove the interaction between the droplet and its periodic image. A structureless surface is located at the bottom of the simulation cell and a stack of 8000 water molecules is positioned on the surface. The top of simulation cell is enclosed with a single graphene layer. Two dimensional periodic boundary condition is applied to the directions that are parallel to the surface plane.

The potential energy is assumed to be pairwise additive, and the potential energy of system Φ is given by

$$\Phi = \sum_i \sum_{j>i} \phi_{ij} + \sum_i \phi_{\mathrm{ws},i} \tag{1}$$

where ϕ_{ij} is the potential energy arising from the interaction between two particles,

$$\phi_{ij} = 4\varepsilon \left(\left[\frac{\sigma}{r_{ij}} \right]^{12} - \left[\frac{\sigma}{r_{ij}} \right]^{6} \right) + \frac{Z_i Z_j}{r_{ij}} \tag{2}$$

and $\phi_{\mathrm{ws},i}$ is the potential energy arising from the interaction between a water molecule with the structureless surface, which is modeled by

$$\phi_{\mathrm{ws},i} = \frac{4}{3}\pi\rho_s\varepsilon_{\mathrm{ws}}\sigma_{ws}^3 \left[\frac{2}{15}\left(\frac{\sigma_{\mathrm{ws}}}{r_{\perp,i}} \right)^9 - \left(\frac{\sigma_{\mathrm{ws}}}{r_{\perp,i}} \right)^3 \right] \tag{3}$$

where $\rho_s (= 66\,\mathrm{nm}^{-3})$ is the "atomic" density of the surface, $r_{\perp,i}$ is the normal distance of the i-th water molecule from the surface plane, σ_{ws} and $\varepsilon_{\mathrm{ws}}$ are the combined Lennard-Jones parameters from the water potential model and the surface model obtained using the Lorentz-Berthelot mixing rule as

$$\sigma_{\mathrm{ws}} = \frac{\sigma_{\mathrm{w}} + \sigma_{\mathrm{s}}}{2} \tag{4}$$

$$\varepsilon_{\mathrm{ws}} = \lambda (\varepsilon_{\mathrm{w}}\varepsilon_{\mathrm{s}})^{1/2} \tag{5}$$

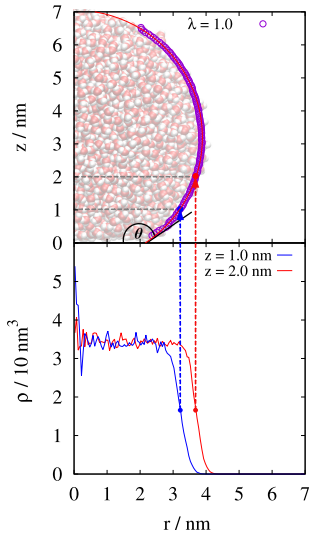

Figure 1 Liquid-gas interface (top) determined from the local density of horizontal layers of water droplet (bottom). The location of liquid-gas interface is defined as the distance r where the local density falls into half and a curve is fitted using the circular least square method. The contact angle θ is calculated from the tangent line of the curve at $z = 0$.

where σ_{s} and ε_{s} are the Lennard-Jones parameters whose values are opted from Ref. 33 for modelling the surface of a graphite. Here a scaling constant λ is introduced to modify the hydrophilicity of the surface and, thus, to alter the contact angle of water droplet. The description of interactions between water molecules is varied using SPC/E[34], TIP4P[35], and TIP5P[36] potential models.

2.2 Molecular dynamics simulations

MD simulations at constant temperature and volume are performed using GROMACS 4.6.5[45,46]. The equation of motion is integrated using the leapfrog algorithm at 2 fs time step. The potential energy arising from the interaction between two particles is smoothly truncated at (r_{cut} =) 8.65 Å using a switching function that takes effect from 6.65 Å. The cutoff distance is chosen to be far beyond the radius of first and second coordination shell of pure water that are typically around 3 Å and 4.5 Å, respectively, as reported by both simulation and experimental works[47]. Nosé-Hoover thermostat is applied to keep the simulation temperature at 298 K with a coupling time of 0.5 ps[48,49]. The geometry of a water molecule is constrained using SETTLE algorithm[50]. The position of all carbon atoms in the graphene layer at the top of simulation cell is fixed during the simulation. The system is equilibrated for 1 ns and the trajectory of water molecules is sampled from the 39 ns production run.

3 Results and discussion

The contact angle is calculated from the liquid-gas interfacial line determined using a cylindrical binning procedure followed by the circular least square fitting[29,33,41–43]. In this method, for each configuration snapshot, the liquid droplet is divided into several horizontal layers. The layer thickness is chosen to be 0.5 Å to ensure that each layer contains enough water molecules to give

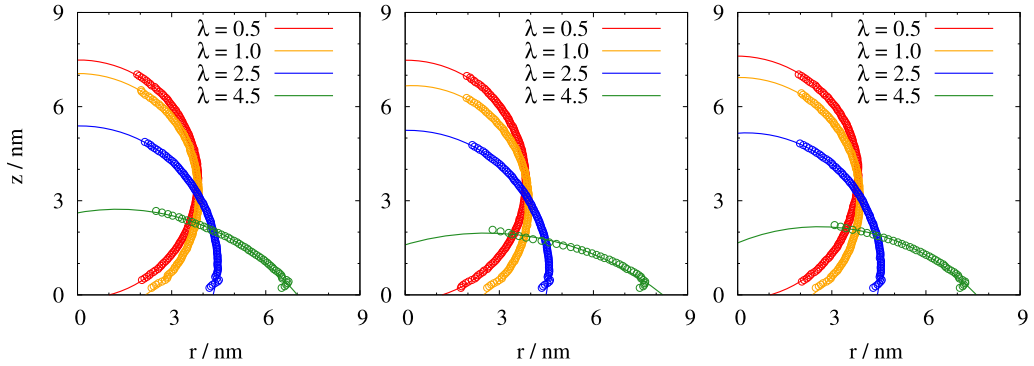

Figure 2 Liquid-gas interfaces of water droplets, that interacts with SPC/E (left), TIP4P (middle), and TIP5P (right) potential models, and their fitted curves at various water-surface interaction scaling factors λ. The liquid-gas interfaces near the top of water droplet are omitted due to the scarce number of water molecules that leads to poor statistics.

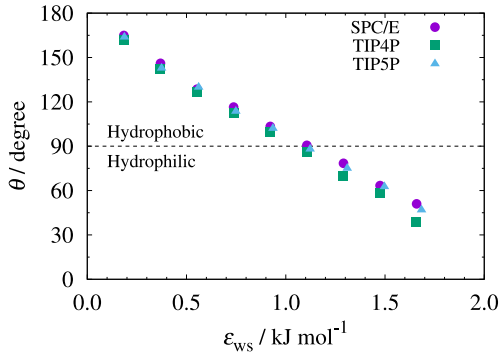

Figure 3 Contact angles of water droplets on a structureless surface at various water-surface interaction parameters ε_{ws} defined in Eq. 5. Three potential models for describing the interactions between water molecules: SPC/E, TIP4P, and TIP5P, are adopted for comparison. The contact angles are calculated from the liquid-gas interfacial line. By definition, the surface is hydrophobic when $\theta > 90°$ and is hydrophilic otherwise.

a uniform density. The center of symmetry of each layer is taken from the lateral position of the center of mass of the droplet. The local density $\rho_l(r)$ as a function of the distance to the center of symmetry r is then calculated by applying cylindrical binning and averaged over the time. The location of liquid-gas interface of this layer is then defined as the distance r where the density falls into half, as shown in Figure 1.

The liquid-gas interfacial lines that corresponds to the shape of water droplets on a structureless surface are shown in Figure 2. The strength of water-surface interactions, described by ε_{ws} parameter in Eq. 3, is modified using a scaling factor λ according to the Eq. 5. The surface is shown to be hydrophobic at small λ and hydrophilic at high λ. The droplet shapes are seemed to be invariant to the water potential models at $\lambda = 0.5$ and 2.5, but a difference in droplet radius is observed at $\lambda = 4.5$ where SPC/E gives the smallest droplet radius and TIP4P gives the largest. Since the number of water molecule N_w is identical, larger droplet radius indicates that the wetting of surface is improved and a smaller contact angle can be expected.

Figure 3 shows the comparison of contact angles θ of water droplets obtained from MD simulations using three different potential models of water at various levels of surface hydrophilicity. On this structureless surface, the boundary of hydrophobic/hydrophilic is observed when ε_{ws} is $\sim 1.1\,\mathrm{kJ\,mol^{-1}}$ for all the studied water potential models. The differences in contact angle between three potential models become more visible as the surface become more hydrophilic with the increase of ε_{ws}. In accordance to Figure 2, water droplets described by TIP4P potential model have the smallest contact angle over the studied ε_{ws}, and SPC/E potential model have the largest contact angle. This trend persists across the variation of surface hydrophilicity. The ability of water to wet the surface can be related to the competition of intermolecular interactions between water-water and water-surface. Since SPC/E model is known to have a negatively large potential energy of water-water interaction Φ_{ww}, as shown in Figure 4, it is straightforward to argue that the water molecules of this model prefer to stay in the droplet phase, thus lower their tendency to wet the surface. However, when comparing between TIP4P and TIP5P potential models, the trend of contact angle does not always follow the trend of Φ_{ww}. For all models, the trend of contact angle resembles the trend of potential energy of water-surface interaction Φ_{ws} as shown in Figure 4; thus, further emphasizes the importance of parametrization water-surface interaction in accordance to the known experimental facts[29,33].

Another method to calculate the contact angle is based on a spherical geometry approximation that relates the contact angle θ with the average height of the center of mass of the water droplet h_{CoM} according to[27,32,44]

$$\langle h_{CoM} \rangle = (2)^{-4/3} R_0 \left(\frac{1-\cos\theta}{2+\cos\theta} \right)^{1/3} \frac{3+\cos\theta}{2+\cos\theta} \qquad (6)$$

where $R_0 (= 3N/4\pi\rho_0)$ is the radius of a spherical drop of N water molecules at a uniform density ρ_0 and the bracket $\langle \ldots \rangle$ denotes the ensemble average. The method is less tedious since $\langle h_{CoM} \rangle$ can be obtained immediately from the simulations. The contact angles obtained using this method are shown in Figure 5. When compared to the results from the liquid-gas interfacial line method, the center of mass method tends to give a higher value of contact angles, regardless of the adopted potential models of

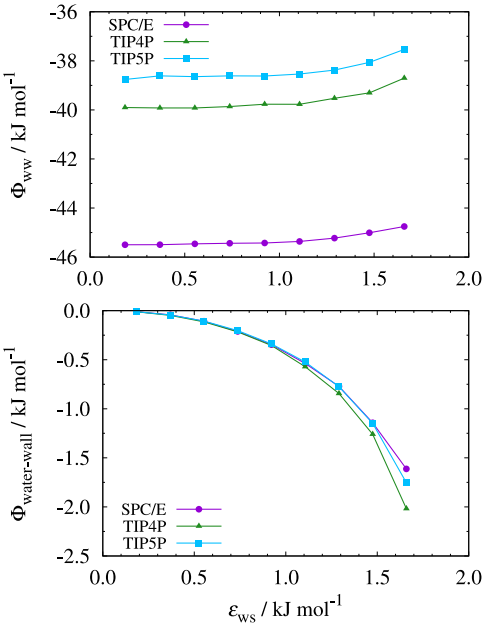

Figure 4 Potential energy arising from the interaction between water-water (top) and water-surface (bottom) at various water-surface interaction parameters ε_{ws} defined in Eq. 5. Three potential models for describing the interactions between water molecules: SPC/E, TIP4P, and TIP5P, are adopted for comparison.

water. Nevertheless, both methods are in agreement for the gradient line of $\Delta\theta/\Delta\varepsilon_{ws}$ and, thus, the center of mass method can be useful for a rapid assessment of contact angle of water droplet at various surface properties.

4 Conclusion

MD simulations of water droplet on a structureless surface have been performed to investigate the sensitivity of contact angle calculation to the adopted potential models of water. The investigation is carried out over the variation of surface hydrophilicity by introducing a scaling factor λ that modify the strength of water-surface interaction through ε_{ws} parameter. Under a similar thermodynamics condition, the computed results shows that SPC/E model gives the largest contact angle, while TIP4P gives the smallest. This trend persists over all the studied variation of surface hydrophilicity. The difference in contact angle between potential models become more visible as the hydrophilicity of surface increases. Although the large contact angle for SPC/E can be argued by its negatively large potential energy of water-water interaction, the trend of contact angle between TIP4P and TIP5P resembles more to the trend of potential energy of water-surface interaction. An alternative method to compute a contact angle based on the height of center-of-mass of the droplet is shown to reproduce the contact angle trend with the change of surface hydrophilicity, although the method generally gives a larger contact angles compared to those obtained from liquid-gas interfacial line.

Acknowledgements

This work is supported by the Directorate of Research and Community Service, under the Indonesian Ministry of Research, Technology, and Higher Education, through PDUPT funding scheme. The authors are grateful for the support.

References

1 M. Liu, S. Wang and L. Jiang, Nature-inspired superwettability systems, *Nature Reviews Materials*, 2017, **2**, 17036.

2 Y. Zheng, H. Bai, Z. Huang, X. Tian, F.-Q. Nie, Y. Zhao, J. Zhai and L. Jiang, Directional water collection on wetted spider silk, *Nature*, 2010, **463**, 640–643.

3 A. R. Parker and C. R. Lawrence, Water capture by a desert beetle, *Nature*, 2001, **414**, 33–34.

4 J. Iturri, L. Xue, M. Kappl, L. García-Fernández, W. J. P. Barnes, H.-J. Butt and A. del Campo, Torrent Frog-Inspired Adhesives: Attachment to Flooded Surfaces, *Advanced Functional Materials*, 2015, **25**, 1499–1505.

5 Y. Huang, Y. Hu, C. Zhu, F. Zhang, H. Li, X. Lu and S. Meng, Long-Lived Multifunctional Superhydrophobic Heterostructure Via Molecular Self-Supply, *Advanced Materials Interfaces*, 2016, **3**, 1500727.

6 H. Bellanger, T. Darmanin, E. Taffin de Givenchy and F. Guittard, Chemical and Physical Pathways for the Preparation of Superoleophobic Surfaces and Related Wetting Theories, *Chemical Reviews*, 2014, **114**, 2694–2716.

7 R. Blossey, Self-cleaning surfaces - Virtual realities, *Nature Materials*, 2003, **2**, 301–306.

8 E. Vazirinasab, R. Jafari and G. Momen, Application of superhydrophobic coatings as a corrosion barrier: A review, *Surface and Coatings Technology*, 2018, **341**, 40–56.

9 Y. Taga, Recent progress in coating technology for surface modification of automotive glass, *Journal of Non-Crystalline Solids*, 1997, **218**, 335–341.

10 J. Yong, J. Huo, F. Chen, Q. Yang and X. Hou, Oil/water separation based on natural materials with super-wettability: recent advances, *Physical Chemistry Chemical Physics*, 2018, **20**, 25140–25163.

11 M. Lampin, R. Warocquier-Clerout, C. Legris, M. Degrange and M. F. Sigot-Luizard, Correlation between substratum roughness and wettability, cell adhesion, and cell migration, *Journal of Biomedical Materials Research*, 1997, **36**, 99–108.

12 K. Ichimura, Light-Driven Motion of Liquids on a Photoresponsive Surface, *Science*, 2000, **288**, 1624–1626.

13 J. Lahann, A Reversibly Switching Surface, *Science*, 2003, **299**, 371–374.

14 M. Brehm, J. M. Scheiger, A. Welle and P. A. Levkin, Reversible Surface Wettability by Silanization, *Advanced Materials Interfaces*, 2020, **7**, 1–8.

15 M. Voué and J. De Coninck, Spreading and wetting at the microscopic scale: Recent developments and perspectives, *Acta Materialia*, 2000, **48**, 4405–4417.

16 D. Brutin and V. Starov, Recent advances in droplet wetting and evaporation, *Chemical Society Reviews*, 2018, **47**, 558–

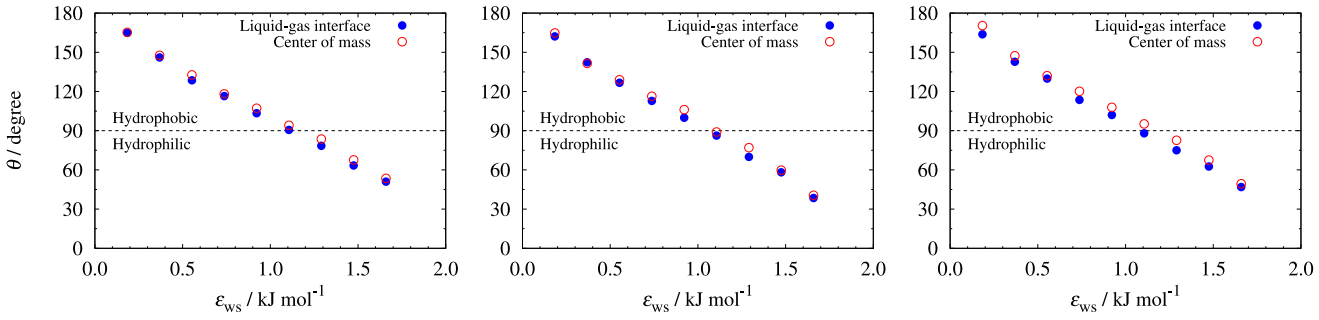

Figure 5 Comparison between contact angles calculated from the height of center of mass of droplet with those calculated from the liquid-gas interfacial line. Data from the latter method are actually the same with Figure 3, but they are included here to make the comparison easier. The interaction between water molecules are modelled with: SPC/E (left), TIP4P (middle), and TIP5P (right).

585.

17 Y. Gao, C. Zhu, C. Zuhlke, D. Alexander, J. S. Francisco and X. C. Zeng, Turning a superhydrophilic surface weakly hydrophilic: Topological wetting states, *Journal of the American Chemical Society*, 2020, **142**, 18491–18502.

18 V. Khosravi, S. M. Mahmood, D. Zivar and H. Sharifigaliuk, Investigating the applicability of molecular dynamics simulation for estimating the wettability of sandstone hydrocarbon formations, *ACS Omega*, 2020, **5**, 22852–22860.

19 A. Silvestri, E. Ataman, A. Budi, S. L. Stipp, J. D. Gale and P. Raiteri, Wetting Properties of the CO2-Water-Calcite System via Molecular Simulations: Shape and Size Effects, *Langmuir*, 2019, **35**, 16669–16678.

20 F. Ghalami, T. Sedghamiz, E. Sedghamiz, F. Khashei and E. Zahedi, Molecular Dynamics Simulation of Wetting and Interfacial Properties of Multicationic Ionic Liquid Nanodroplets on Boron Nitride Monolayers: A Comparative Approach, *Journal of Physical Chemistry C*, 2019, **123**, 13551–13560.

21 S. Gim, H. K. Lim and H. Kim, Multiscale Simulation Method for Quantitative Prediction of Surface Wettability at the Atomistic Level, *Journal of Physical Chemistry Letters*, 2018, **9**, 1750–1758.

22 M. Khalkhali, H. Zhang and Q. Liu, Effects of Thickness and Adsorption of Airborne Hydrocarbons on Wetting Properties of MoS2: An Atomistic Simulation Study, *Journal of Physical Chemistry C*, 2018, **122**, 6737–6747.

23 S. W. Hung and J. Shiomi, Dynamic Wetting of Nanodroplets on Smooth and Patterned Graphene-Coated Surface, *Journal of Physical Chemistry C*, 2018, **122**, 8423–8429.

24 S. Gao, Q. Liao, W. Liu and Z. Liu, Effects of Solid Fraction on Droplet Wetting and Vapor Condensation: A Molecular Dynamic Simulation Study, *Langmuir*, 2017, **33**, 12379–12388.

25 S. Malali and M. Foroutan, Study of Wetting Behavior of BMIM+/PF6- Ionic Liquid on TiO2 (110) Surface by Molecular Dynamics Simulation, *Journal of Physical Chemistry C*, 2017, **121**, 11226–11233.

26 M. Khalkhali, N. Kazemi, H. Zhang and Q. Liu, Wetting at the nanoscale: A molecular dynamics study, *Journal of Chemical Physics*, 2017, **146**, 1–12.

27 L. Hakim, W. Dita Saputri and S. M. Ulfa, Molecular dynamics simulation of a reversible hydrophobic-hydrophilic functionalized surface, *2016 International Electronics Symposium (IES)*, 2016, 215–218.

28 S. Chen, J. Wang, T. Ma and D. Chen, Molecular dynamics simulations of wetting behavior of water droplets on polytetrafluorethylene surfaces, *The Journal of Chemical Physics*, 2014, **140**, 114704.

29 Y. Wu and N. R. Aluru, Graphitic carbon-water nonbonded interaction parameters, *Journal of Physical Chemistry B*, 2013, **117**, 8802–8813.

30 A. Shahraz, A. Borhan and K. A. Fichthorn, Wetting on physically patterned solid surfaces: The relevance of molecular dynamics simulations to macroscopic systems, *Langmuir*, 2013, **29**, 11632–11639.

31 Q. Yuan and Y.-P. Zhao, Wetting on flexible hydrophilic pillar-arrays, *Scientific Reports*, 2013, **3**, 3–8.

32 J. T. Hirvi and T. a. Pakkanen, Molecular dynamics simulations of water droplets on polymer surfaces, *The Journal of Chemical Physics*, 2006, **125**, 144712.

33 T. Werder, J. H. Walther, R. L. Jaffe, T. Halicioglu and P. Koumoutsakos, On the water-carbon interaction for use in molecular dynamics simulations of graphite and carbon nanotubes, *Journal of Physical Chemistry B*, 2003, **107**, 1345–1352.

34 H. J. Berendsen, J. R. Grigera and T. P. Straatsma, The missing term in effective pair potentials, *Journal of Physical Chemistry*, 1987, **91**, 6269–6271.

35 W. L. Jorgensen, J. Chandrasekhar, J. D. Madura, R. W. Impey and M. L. Klein, Comparison of simple potential functions for simulating liquid water, *The Journal of Chemical Physics*, 1983, **79**, 926–935.

36 M. W. Mahoney and W. L. Jorgensen, A five-site model for liquid water and the reproduction of the density anomaly by rigid, nonpolarizable potential functions, *The Journal of Chemical Physics*, 2000, **112**, 8910.

37 E. Sanz, C. Vega, J. Abascal and L. MacDowell, Phase Diagram of Water from Computer Simulation, *Physical Review Letters*, 2004, **92**, 23–26.

38 M. W. Mahoney and W. L. Jorgensen, Diffusion constant of the TIP5P model of liquid water, *The Journal of Chemical Physics*,

2001, **114**, 363.

39 C. Vega and J. L. Abascal, Simulating water with rigid non-polarizable models: A general perspective, *Physical Chemistry Chemical Physics*, 2011, **13**, 19663–19688.

40 C. Vega, Water: One molecule, two surfaces, one mistake, *Molecular Physics*, 2015, **113**, 1145–1163.

41 T. D. Blake, A. Clarke, J. De Coninck and M. J. De Ruijter, Contact angle relaxation during droplet spreading: Comparison between molecular kinetic theory and molecular dynamics, *Langmuir*, 1997, **13**, 2164–2166.

42 M. J. de Ruijter, T. D. Blake and J. De Coninck, Dynamic wetting studied by molecular modeling simulations of droplet spreading, *Langmuir*, 1999, **15**, 7836–7847.

43 G. Scocchi, D. Sergi, C. D'Angelo and A. Ortona, Wetting and contact-line effects for spherical and cylindrical droplets on graphene layers: A comparative molecular-dynamics investigation, *Physical Review E*, 2011, **84**, 061602.

44 J. Hautman and M. L. Klein, Microscopic Wetting Phenomena, *Physical Review Letters*, 1989, **6762**, 1763–1766.

45 B. Hess, C. Kutzner, D. Van Der Spoel and E. Lindahl, GROMACS 4: Algorithms for highly efficient, load-balanced, and scalable molecular simulation, *Journal of Chemical Theory and Computation*, 2008, **4**, 435–447.

46 M. J. Abraham, T. Murtola, R. Schulz, S. Páll, J. C. Smith, B. Hess and E. Lindah, Gromacs: High performance molecular simulations through multi-level parallelism from laptops to supercomputers, *SoftwareX*, 2015, **1-2**, 19–25.

47 G. Camisasca, H. Pathak, K. T. Wikfeldt and L. G. M. Pettersson, Radial distribution functions of water: Models vs experiments, *The Journal of Chemical Physics*, 2019, **151**, 044502.

48 S. Nosé, A unified formulation of the constant temperature molecular dynamics methods, *The Journal of Chemical Physics*, 1984, **81**, 511–519.

49 W. G. Hoover, Canonical dynamics: Equilibrium phase-space distributions, *Physical Review A*, 1985, **31**, 1695–1697.

50 S. Miyamoto and P. A. Kollman, Settle: An analytical version of the SHAKE and RATTLE algorithm for rigid water models, *Journal of Computational Chemistry*, 1992, **13**, 952–962.